Biogeochemistry (2010) 97:211–229
DOI 10.1007/s10533-009-9368-y

# An assessment of karstic submarine groundwater and associated nutrient discharge to a Mediterranean coastal area (Balearic Islands, Spain) using radium isotopes

**E. Garcia-Solsona · J. Garcia-Orellana · P. Masqué · E. Garcés · O. Radakovitch · A. Mayer · S. Estradé · G. Basterretxea**

Received: 2 September 2008 / Accepted: 15 August 2009 / Published online: 11 September 2009


**Abstract** Short and long-lived radium isotopes ($^{223}$Ra, $^{224}$Ra, $^{226}$Ra, $^{228}$Ra) were used to quantify submarine groundwater discharge (SGD) and its associated input of inorganic nitrogen ($NO_3^-$), phosphorus ($PO_4^{3-}$) and silica ($SiO_4^{4-}$) into the karstic Alcalfar Cove, a coastal region of Minorca Island (Western Mediterranean Sea). Cove water, seawater and groundwater (wells and karstic springs) samples were collected in May 2005 and February 2006 for radium isotopes and in November 2007 for dissolved inorganic nutrients. Salinity profiles in cove waters suggested that SGD is derived from shallow brackish springs that formed a buoyant surface fresh layer of only 0.3 m depth. A binary mixing model that considers the distribution of radium activities was used to determine the cove water composition. Results showed that cove waters contained 20% brackish groundwater; of which 6% was recirculated seawater and 14% corresponded to freshwater discharge. Using a radium-derived residence time of 2.4 days, a total SGD flux of 150,000 $m^3$ $year^{-1}$ was calculated, consisting of 45,000 $m^3$ $year^{-1}$ recirculated seawater and 105,000 $m^3$ $year^{-1}$ fresh groundwater. Fresh SGD fluxes of $NO_3^-$, $SiO_4^{4-}$ and $PO_4^{3-}$ were estimated to be on the order of 18,000, 1,140 and 4 μmol $m^{-2}$ $day^{-1}$, respectively, and presumably sustain the high phytoplankton biomass observed in the cove during summer. The total amount of $NO_3^-$ and $SiO_4^{4-}$ supplied by SGD was higher than the measured inventories in the cove, while the reverse was true for $PO_4^{3-}$. These discrepancies are likely due to non-conservative biogeochemical processes that occur within the subterranean estuary and Alcalfar Cove waters.

**Keywords** Groundwater discharge · Inorganic nutrients · Karstic springs phytoplankton proliferations · Radium isotopes

E. Garcia-Solsona (✉) · J. Garcia-Orellana · P. Masqué
Departament de Física, Institut de Ciència i Tecnologia Ambientals (ICTA), Universitat Autònoma de Barcelona, 08193 Cerdanyola del Valles, Spain
e-mail: Esther.Garcia@uab.es

J. Garcia-Orellana
School of Marine and Atmospheric Sciences, Stony Brook University, Stony Brook, NY 11794-5000, USA

E. Garcés
Departament de Biologia Marina i Oceanografia, Institut de Ciències del Mar-CMIMA, CSIC, P. Marítim de la Barceloneta, 37-43, 08003 Barcelona, Spain

O. Radakovitch · A. Mayer
CEREGE-Université Paul Cézanne Aix Marseille III, Europole de l'Arbois, BP 80, 13545 Aix en Provence, France

S. Estradé
Institut Menorquí d'Estudis (IME-OBSAM), Camí des Castell 28, 07002 Mahon, Minorca, Spain

G. Basterretxea
Institut Mediterrani d'Estudis Avançats (IMEDEA), Consell Superior d'Investigacions Cientifigues (CSIC-UIB), Miquel Marques 21, 97190 Esporles, Majorca, Spain

## Introduction

A common problem encountered when determining coastal hydrological mass balances and their related impacts on marine ecosystems is the evaluation of the water flux and the associated chemical load of the submarine groundwater discharge (SGD) to the coastal ocean. Several previous studies have demonstrated that groundwater discharge (including both terrestrially-derived fresh groundwater and recirculated seawater; Burnett et al. 2006) constitutes an important water source in various coastal environments around the world (Rama and Moore 1996; Corbett et al. 2000; Burnett et al. 2003).

Although limited, several recent studies have focused on SGD as a vector for nutrient input into coastal regions (Garrison et al. 2003; Slomp and Cappellen 2004; Paytan et al. 2006). Depending on water-table and hydraulic recharge characteristics, the influence of groundwater as a source of new nutrients can extend from highly localized to regional scales (e.g. the U.S. western Atlantic continental shelf; Capone and Bautista 1985; Moore 1996). These effects may further change with time as SGD may be substantially modified by human population growth and agricultural practices that not only increase nutrient loadings (and hence eutrophication, Nixon 1995), but also influence nutrient ratios. Such changes in nutrient biogeochemistry may ultimately alter community structure, and stimulate growth and even production of harmful taxa (Anderson et al. 2002, Hallegraeff 1993; Glibert et al. 2008, Maso and Garcés 2006).

Karstic regions represent $\sim$15% of the Earth's land surface and comprise 60% of the Mediterranean shoreline (UNESCO 2004). In these areas, rainfall easily penetrates into the aquifer through permeable carbonate outcrops and fractures. Since groundwater inside the aquifer dissolves the limestone and creates preferential conduits, groundwater may flow more rapidly than in porous or detritic homogeneous aquifers (Cable et al. 2002; UNESCO 2004). Indeed, regions comprised of carbonate rocks are often an abundant source of local water (LaMoreaux and LaMoreaux 2007). Furthermore, these waters are likely to be substantially enriched in other components as karstic springs have minimal filtering or alteration of the load by soils or sediments. Whether or not karstic springs are brackish, which changes the ionic potential of the water and hence the chemical composition, is influenced by differences between fresh and seawater densities and the venturi effect (Maramathas et al. 2006).

The southern shore of Minorca is an example of a classic karstic setting as it is characterized by narrow, small coves with restricted water circulation. Like many other coastal areas in the Mediterranean Sea, Minorca has an intense demand for its water resources due to increased population and tourism. There are no rivers or dams, and thus, water for human consumption and agriculture is mainly extracted from wells that are recharged via precipitation (Trilla 1979). Subsequently, groundwater quality is affected by nutrient loading from fertilization, cattle farming, and increasing urbanization of the coastal areas. Combined with reduced mixing in the summer, SGD likely promotes substantial increases in both inorganic and organic nutrients in some coastal areas that may lead to an increase in nuisance or even toxic algae (Basterretxea et al. 2005, 2007). However, there is an actual lack of SGD measurements in the region.

Over the past decade, new indirect methods have emerged that attempt to overcome the inherent difficulties of direct SGD flux measurements. These include the radium isotopic quartet ($^{223}$Ra, $^{224}$Ra, $^{226}$Ra and $^{228}$Ra), which has been successfully applied in numerous SGD studies to determine both water and nutrient inputs (e.g. Moore 1999; Charette et al. 2001; Hwang et al. 2005; Charette and Scholten 2008). This previous research has found that, depending on a number of factors such as aquifer rock composition, water residence time, salinity, redox potential, and the presence of iron and manganese (hydr)oxides, Ra isotopes can be enriched in groundwater by over an order of magnitude relative to coastal waters. As a result, using the Ra distribution measured in coastal waters enables a Ra mass balance to be built that evaluates SGD and associated component fluxes, such as nutrients (Charette and Buesseler 2004).

The aim of this study is to estimate the SGD flux into the karstic cove of Alcalfar (Minorca, Balearic Islands) using the radium mass balance approach. This coastal environment is of particular interest to SGD studies because cove waters are fresher than many other places around the island and prone to eutrophication and phytoplankton blooms. We attempt to determine the SGD-associated nutrient

inputs to evaluate the potential connection between the groundwater flux and recurrent algal blooms that occur in this area.

## Study site

Minorca is located in the western Mediterranean Sea (Fig. 1) and is the second largest island in the Balearic archipelago, with a total surface area of 700 $km^2$. Mean rainfall is $\sim$600 mm $year^{-1}$, with maxima occurring in the spring and autumn, and minima during the summer. The island is divided into two geomorphological settings: an impermeable region located in the north and a more permeable band that consists of the main aquifer (*Migjorn*) in the south (Fornós et al. 2004) (Fig. 1). This southern region (365 $km^2$) is characterized by a highly eroded and karstified carbonate plain of Miocene origin that dips slightly towards the sea. Hence, the plain has deep ravines ending in small, narrow coves. Aquifer permeability increases towards the coast due to the major karstic development (Fayas 1972).

The unconfined Migjorn aquifer supplies up to 90% of the water on the island ($\sim 11 \times 10^6$ $m^3$ $year^{-1}$), with most of the water used for human consumption and agriculture. The aquifer is an open system with diffuse or direct water discharge through subterranean exits to the sea or concentrated in the ravines located in the central sector (Barón et al. 1979). It can be divided into three sectors according to their hydrological characteristics (Bourrouilh 1983). The eastern and western zones have a high permeability (up to 25 m $day^{-1}$) with soft hydraulic gradients (less than 0.4%) close to the sea level. This allows seawater intrusion to occur in precisely the same areas where population growth and thus, groundwater extraction, are higher. In contrast, the central zone constitutes a tectonic block furrowed into many fluvial valleys. It is characterized by low permeability (0.1 m $day^{-1}$) and higher (2%) hydraulic gradients. Hydrological mass balances for the aquifer suggest that fresh groundwater discharge ranges from $17 \times 10^6$ to $37 \times 10^6$ $m^3$ $year^{-1}$ (Estradé 2005).

The Alcalfar Cove is located in the south-eastern corner of Minorca in the main aquifer (Fig. 1). This

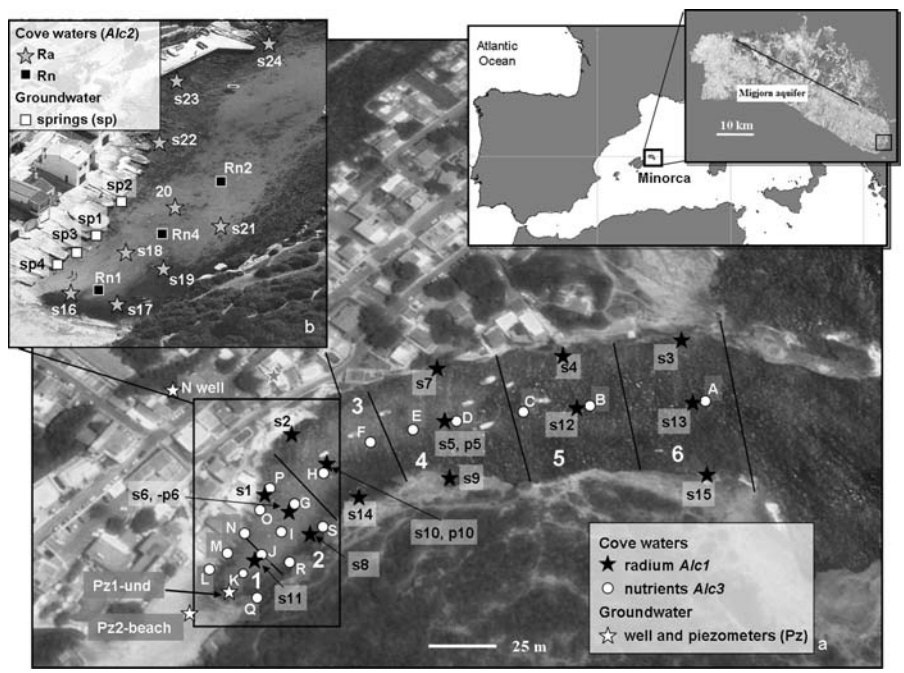


**Fig. 1** Sampling stations in the studied area covering **a** the whole cove (Alc1 in May 2005 and Alc3 in November 2007) and **b** centered at the major coast (fisher quays; Alc2 in February 2006). Coastal and open seawater samples are not shown. The six *boxes* in which the cove has been divided are also indicated (1–6). Also, a general map of the western Mediterranean Sea showing Minorca location and its N–S partition in two hydrological settings (*inset*) is depicted with the location of the Alcalfar Cove indicated by the *square*

cove is typical of the narrow, semi-enclosed karstic inlets found in the eastern coast of the Island. It is 275 m long, 60 m wide (1.65 ha), and ×8 m deep at the outermost cove boundary. Although surrounded by an urbanized watershed, there are many isolated residences with old septic tanks, not yet connected to a municipal sanitary network. There is no riverine or stream input into the cove. However, some brackish submarine springs have been visually identified in the northern side. The beach is artificial, with sand deposited from deeper ocean regions, resulting in a thin sandy sediment layer of approximately 0.5 m depth overlaying the permeable limestone.

## Sampling and methods

### Field surveys

Three specific sampling campaigns were carried out at Alcalfar Cove: *Alcalfar 1* (Alc1) on May 2005, *Alcalfar 2* (Alc2) on February 2006 and *Alcalfar 3* (Alc3) on November 2007 (Fig. 1). During Alc1 and Alc3, samples were collected at stations throughout the entire cove area. The winter fieldwork of Alc2, however, was mainly focused on the inner cove, close in proximity to the old fisher quays and springs. Temperature and salinity measurements were recorded in the field for all samples using an YSI-30 probe. In addition, vertical profiles of salinity and temperature were conducted at several stations along a transect within the cove to 250 m offshore in March 2007 using a portable sensor (YSI-6000 XLS) in order to determine the region of the water column influenced by SGD in the cove.

During Alc1 (May 2005), 15 surface water samples were collected from the cove (volume of 50 l; sites s1–s15, Fig. 1a), as well as four submarine springs (20–50 l; Sp 1–4, Fig. 1b), coastal and open seawater samples (400 and 1,000 m from the cove inlet, respectively; 50 l, location not shown) and one well (100 l, *N well*, located at 80 m from the coast, Fig. 1a). During the second survey campaign (Alc2; February 2006), water samples were obtained from nine stations in the cove (50 l; sites s16–s24, Fig. 1b), two piezometers (one underwater -*Pz1-und*- and one on the beach sand -*Pz2-beach*-) (20 l, Fig. 1a), one submarine spring (20 l; Sp4, Fig. 1b) and two wells (50 l; *P1* and *P2 wells*, located 400 m inland from the coast, locations not shown). A submersible pump was used to collect water from the springs and wells. Porewater Ra profiles were sampled at 45 cm depth at two locations using the Retract-A-Tip piezometer system (AMS, Inc.) described by Charette and Allen (2006) and connected to a peristaltic pump. Wells were emptied twice prior to sample collection to ensure that representative groundwaters were collected.

Radon measurements performed on February 2006 (Alc2) were obtained for surface waters (at 15 cm depth; *Rn4*, Fig. 1b) and near bottom waters (at 15 cm above the sea floor; *Rn1* and *Rn2*, Fig. 1b) of the cove, as well as from one of the submarine springs (*sp2*, Fig. 1b), two piezometers (*Pz1-und* and *Pz2-beach*) and a well (*N well*).

Sampling during November 2007 (Alc3) focused on nutrients and consisted of 19 stations within the cove (sites A–S, Fig. 1a), and two samples from the *N well*. Polypropylene bottles of 60 ml capacity were rinsed three times prior to water collection and were immediately frozen (−20°C) for subsequent analyses in the laboratory. Additional information on nutrients and phytoplankton biomass in the nearshore (∼1 m depth) was obtained from a water quality monitoring program on the island conducted during the summers of 2005 and 2006, in which surface nutrient, temperature, salinity and chlorophyll *a* were measured at 26 coves around Minorca. These samples provide a general context of the conditions in the region.

### Radium analyses

Water samples for Ra analysis were filtered at <1 l $min^{-1}$ through manganese impregnated acrylic fiber (hereafter, Mn-fiber) to quantitatively extract the radium isotopes (Moore 1976; Moore et al. 1995). After filtering and once in the laboratory, the Mn-fibers were rinsed with deionized water and partially dried with compressed air until the water-to-fiber ratio reached the range 0.3–1.2 $g_{H_2O}/g_{fiber}$ (Sun and Torgersen 1998; Garcia-Solsona et al. 2008). Then, the samples were measured using a Radium Delayed Coincidence Counter (RaDeCC) to determine the short-lived radium isotopes, $^{223}Ra$ ($T_{1/2}$ = 11.4 days) and $^{224}Ra$ ($T_{1/2}$ = 3.66 days). This detection system measures the delayed coincidence signals generated by the decay of the radon daughters of $^{223}Ra$ and $^{224}Ra$ ($^{219}Rn$ and $^{220}Rn$, respectively) to a short-lived

polonium isotope, $^{215}$Po ($T_{1/2} = 1.8$ ms) and $^{216}$Po ($T_{1/2} = 150$ ms). A more detailed description of how these calculations are performed is provided in Moore and Arnold (1996). The associated uncertainties in Ra activities were estimated following Garcia-Solsona et al. (2008).

After measuring the short-lived Ra isotopes, the Mn-fibers were processed to determine $^{226}$Ra and $^{228}$Ra by gamma spectrometry. The Mn-fibers were incinerated at 820°C for 16 h (Charette et al. 2001). The ashes were ground, blended, transferred to counting vials and aged for 3 weeks prior to measurement with a well-type germanium gamma detector. $^{228}$Ra and $^{226}$Ra were determined through their daughters $^{228}$Ac (photopeak at 911 keV) and $^{214}$Pb (photopeaks at 295 and 351 keV) respectively.

### $^{222}$Rn measurements

Activities of $^{222}$Rn were determined by using two RAD7 (Durridge Co, Inc.) portable monitor spectrometers (Burnett and Dulaiova 2003). Briefly, water samples were passed continuously through an air–water exchanger (RAD AQUA system) with the $^{222}$Rn degassed into a closed air loop. After several minutes, radon in this air is at equilibrium with the radon in water, the ratio being determined from the water temperature. The air is pumped through the radon-in-air monitor that determines $^{222}$Rn activities through the measurement of its alpha-emitting daughters $^{214}$Po and $^{218}$Po. The instrument integrated the data every 30 min, and the total counting time varied from 2 to 3 h. In addition, radon was also analyzed in water samples from the piezometer and the wells; they were pumped into 250 ml bottles and measured with a RAD-7 monitor coupled with the RAD-$H_2O$ accessory (Durridge Co., Inc). The water was purged for five minutes and the air was delivered to the RAD-7 monitor. The $^{222}$Rn concentrations were determined from four counting cycles of 5 min, with a lower limit of detection of about 370 Bq.

### Inorganic nutrients

Dissolved inorganic nutrients (nitrate, nitrite, ammonium, phosphate and silicate) were determined using colorimetric methods and a continuous flow autoanalyzer (ALLIANCE Evolution II). The techniques are based on the procedure described by Grasshoff et al. (1999) for manual analyses of individual samples and slightly modified for automated measurements. The certified minor modifications are associated with practical issues concerning specific autoanalyzer (e.g. adapted proportion of analyte vs reagent) and type of water samples (fresh or saline) analyzed. Chlorophyll concentrations (Chl *a*) from the water quality monitoring program were measured using a Turner Designs fluorometer on 50 ml water samples filtered through a GF/F filter.

## Results

### General environmental conditions in the area

A map of Minorca chlorophyll *a* concentrations from the summers of 2005 and 2006 (water quality monitory program), used here as a proxy of phytoplankton biomass (Fig. 2), reveals two areas of phytoplankton blooms, the western and southeastern coasts, where chlorophyll *a* concentrations of 26 mg m$^{-3}$ were observed (Fig. 2). These elevated regions of phytoplankton biomass include the Alcalfar Cove, where high biomass was consistently observed, along with high inorganic nitrogen concentrations (>7 μmol l$^{-1}$) and reduced salinities (<36.5). In addition, both nutrients (e.g. nitrate) in the Alcalfar Cove during this program were comparable between the two summers (9.75 in 2005 and 7.76 μM in 2006).

### Salinity and temperature in the Alcalfar Cove

Groundwater salinities in Alcalfar Cove vary from low values measured in all wells (from 2.0 to 3.2 at 400 and 80 m far from the shoreline, respectively) to intermediate (brackish) values in coastal porewater (salinities of 24.2 in both piezometers) as well as in the submarine springs (average salinity 24.5 ± 1.7; Table 1). These results indicate that mixing, i.e., seawater intrusion, takes place at some distance inland and that discharge to the coast occurs as a brackish mixture of fresh groundwater and recirculated seawater.

Closer examination of the Alc1 (May 2005) and Alc2 (February 2006) campaigns show that cove surface salinities varied from 30.5 to 37.4 within the inner cove (first 70 m offshore) and between 36.4 and 37.8 in the outer cove (70 m offshore to inlet mouth).

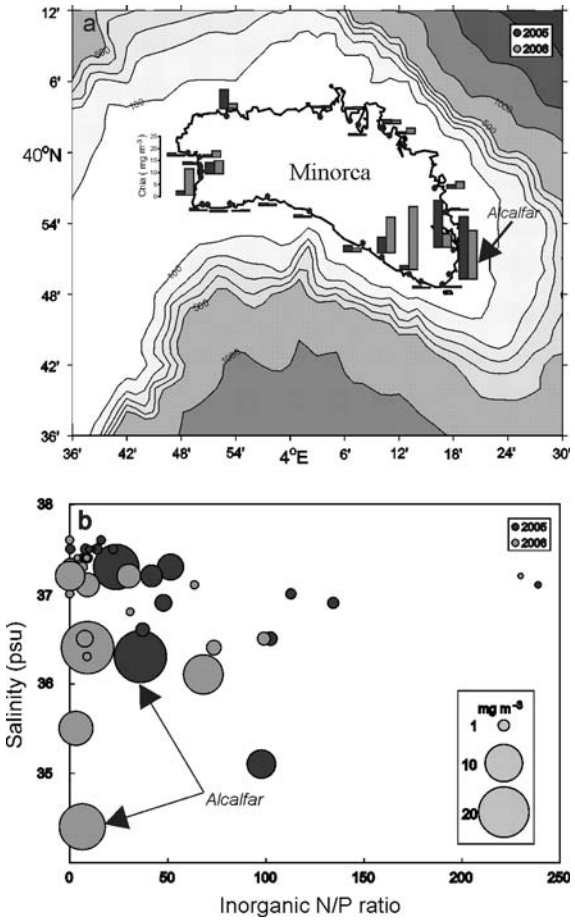


**Fig. 2** **a** Chlorophyll *a* distribution around Minorca with high concentrations in the Alcalfar Cove (*lower right corner*) and **b** inorganic N/P ratios against salinity in the same areas in 2005 and 2006

Average cove water salinities in the overlapped area in May 2005 (35.4 ± 1.4) and February 2006 (35.8 ± 2.6) showed no statistical difference. Temperatures varied from 13.7 to 17.7°C within the inner cove to between 17.0 and 18.0°C in the outer cove. In contrast, the coastal and open seawater samples had salinities of ~38.1 and temperatures of 16.0 (May 2005) and 13.5°C (February 2006). Good correlation between salinity and temperature in the cove and well waters occurred in February 2006 (Alc2; $R^2 = 0.92$, $p < 0.0001$), but no correlation was observed on May 2005 (Alc1; $R^2 = 0.17$, $p = 0.78$). These results are most likely due to the higher difference between coastal seawater and spring groundwater temperatures in February (~4°C) relative to May (~2°C). The latter divergence is probably too small to allow temperature to trace SGD.

During March 2007, the highest salinity (38.5), was ubiquitously detected at 90 cm depth within the transect and offshore (Fig. 3). These salinities decreased with decreasing depth to an average of 38.3 at 40 cm. Salinities decreased even further in the surface waters, suggesting the existence of a buoyant fresher water layer that intensified within 50 m of the shoreline (37.0 at 30 cm depth), coincident with the location of visible submarine springs. Overall, salinity differences between surface and bottom waters varied from 1 to 6 units.

## Radium activities

The activities of radium isotopes for all samples are listed in Table 1. A clear enrichment in radium activities is observed in surface cove waters ($^{223}$Ra: 0.5–3.0 dpm 100 l$^{-1}$; $^{224}$Ra: 5–35 dpm 100 l$^{-1}$ and $^{228}$Ra: 2–12 dpm 100 l$^{-1}$) compared to the coastal sea ($^{223}$Ra: 0.5 ± 0.1 dpm 100 l$^{-1}$; $^{224}$Ra: 1.7 ± 0.5 dpm 100 l$^{-1}$ and $^{228}$Ra: 4.6 ± 0.4 dpm 100 l$^{-1}$), with the exception of $^{226}$Ra (ranging from 5.4 to 19 dpm 100 l$^{-1}$ in the cove, while concentration the coastal sea was 14.4 ± 0.4 dpm 100 l$^{-1}$).

Since sampling stations are not homogeneously distributed within the cove, area-weighted average radium activities need to be calculated ($Ra_{avg}$) for surficial cove waters. To do so, the total area of the cove has been divided into six boxes (Fig. 1; Table 1) and the radium average in surface cove waters calculated as follows (Eq. 1):

$$Ra_{avg} = \frac{\sum_{i=1}^{6} \left( Ra_{avg}^{i} \cdot A_i \right)}{A_{std}} \quad (1)$$

where $i$ stands for the number of each box, $Ra_{avg}^{i}$ is the average radium activity measured in each box, $A_i$ is the area of each box and $A_{std}$ is the total surface of the cove (16,535 m$^2$). Average radium activities in cove waters from both campaigns (May 2005 and February 2006) were determined: $^{223}$Ra = 1.2 ± 0.2 dpm 100 l$^{-1}$, $^{224}$Ra = 10.3 ± 1.2 dpm 100 l$^{-1}$, $^{226}$Ra = 10.6 ± 1.4 dpm 100 l$^{-1}$ and $^{228}$Ra = 5.1 ± 1.2 dpm 100 l$^{-1}$. Salinity measurements were also normalized to account for the heterogeneous distribution of groundwater, resulting in an average value for surface cove waters of 36.7.

**Table 1** Radium activities (dpm 100 $l^{-1}$) and salinity for groundwater, cove and coastal seawater samples. The $^{228}Ra/^{226}Ra$ ratios, the boxes in which the cove has been divided and the area-weighted averages for Ra are also shown. The minimum detection activity (MDA) for $^{228}Ra$ is 1.9 dpm 100 $l^{-1}$

| | Sal | $^{223}Ra$ | $^{224}Ra$ | $^{226}Ra$ | $^{228}Ra$ | $^{228}Ra/^{226}Ra$ | Box |
|---|---|---|---|---|---|---|---|
| *Alcalfar 1 (May 2005)* | | | | | | | |
| Groundwater samples | | | | | | | |
| sp1 | 26.9 | 4.5 ± 0.6 | 46 ± 3 | 16.4 ± 0.4 | 17.3 ± 0.9 | 1.06 ± 0.06 | |
| sp2 | 23.4 | 4.3 ± 0.8 | 54 ± 3 | 16.0 ± 0.5 | 16.7 ± 1.1 | 1.04 ± 0.07 | |
| sp3 | 23.2 | 5.6 ± 1.1 | 58 ± 5 | 15.7 ± 0.3 | 20.4 ± 0.7 | 1.30 ± 0.05 | |
| sp4 | 23.2 | 7.0 ± 1.4 | 67 ± 5 | 14.0 ± 0.6 | 24.6 ± 1.5 | 1.76 ± 0.10 | |
| P1 well | 2 | 7 ± 2 | 38 ± 2 | 42.3 ± 0.5 | 29.6 ± 0.8 | 0.70 ± 0.02 | |
| P2 well | 2 | 4.9 ± 0.8 | 36 ± 2 | 36.3 ± 0.7 | 24.6 ± 1.2 | 0.68 ± 0.03 | |
| Surface cove water samples | | | | | | | |
| s1 | 35.8 | 1.4 ± 0.2 | 13.3 ± 1.0 | 15.5 ± 0.4 | 5.3 ± 0.5 | 0.34 ± 0.03 | 2 |
| s2 | 35.3 | 1.5 ± 0.4 | 16.0 ± 1.1 | 19.4 ± 0.7 | 6.6 ± 0.9 | 0.34 ± 0.05 | 3 |
| s3 | 37.2 | 0.5 ± 0.1 | 6.8 ± 0.9 | 9.0 ± 0.4 | 1.9 ± 0.3 | 0.21 ± 0.03 | 6 |
| s4 | 36.5 | 1.4 ± 0.3 | 12.8 ± 1.0 | 13.3 ± 0.5 | 11.6 ± 0.4 | 0.88 ± 0.04 | 5 |
| s5 | 37.2 | 1.02 ± 0.12 | 6.3 ± 0.7 | 12.5 ± 0.4 | 5.2 ± 0.5 | 0.42 ± 0.04 | 4 |
| s6 | 32.6 | 2.4 ± 0.2 | 18.9 ± 1.4 | 13.2 ± 0.2 | 9.4 ± 0.4 | 0.71 ± 0.03 | 2 |
| s7 | 37.4 | 1.35 ± 0.14 | 8.6 ± 0.7 | 11.0 ± 0.2 | 5.4 ± 0.4 | 0.49 ± 0.03 | 4 |
| s8 | 37.1 | 1.03 ± 0.12 | 11.2 ± 1.2 | 12.0 ± 0.3 | 4.3 ± 0.4 | 0.36 ± 0.04 | 2 |
| s9 | 37.5 | 0.41 ± 0.13 | 6.9 ± 0.6 | 5.4 ± 0.3 | 3.1 ± 0.3 | 0.57 ± 0.07 | 4 |
| s10 | 35.5 | 1.5 ± 0.4 | 13.6 ± 1.4 | 11.4 ± 0.4 | 6.9 ± 0.7 | 0.61 ± 0.06 | 3 |
| s11 | 35.1 | 2.5 ± 0.4 | 20 ± 2 | 16.6 ± 0.5 | 11.4 ± 0.9 | 0.69 ± 0.06 | 1 |
| s12 | 37.0 | 0.96 ± 0.12 | 9.9 ± 1.2 | 13.5 ± 0.4 | 4.1 ± 0.4 | 0.30 ± 0.03 | 5 |
| s13 | 36.4 | 0.9 ± 0.2 | 8.3 ± 0.8 | 9.5 ± 0.3 | MDA | 0.20 ± 0.01 | 6 |
| s14 | 36.5 | 1.7 ± 0.2 | 10.5 ± 1.2 | 10.5 ± 0.4 | 3.9 ± 0.5 | 0.37 ± 0.05 | 3 |
| s15 | 37.8 | 0.80 ± 0.12 | 4.9 ± 0.6 | 9.0 ± 0.4 | MDA | 0.21 ± 0.01 | 6 |
| Seawater samples | | | | | | | |
| Open sea | 38.1 | 0.69 ± 0.09 | 2.6 ± 0.4 | 12.1 ± 0.4 | 5.7 ± 0.5 | 0.47 ± 0.05 | |
| Coastal sea | 38.1 | 0.54 ± 0.09 | 1.7 ± 0.5 | 14.4 ± 0.4 | 4.6 ± 0.4 | 0.32 ± 0.03 | |
| Bottom cove water samples | | | | | | | |
| p5 (4 m) | 37.8 | 1.09 ± 0.13 | 4.8 ± 0.6 | 8.9 ± 0.4 | 5.0 ± 0.6 | 0.56 ± 0.07 | 4 |
| p6 (1.5 m) | 37.7 | 0.88 ± 0.13 | 3.6 ± 0.6 | 9.3 ± 0.3 | 2.5 ± 0.3 | 0.27 ± 0.03 | 2 |
| p10 (3 m) | 37.6 | 0.89 ± 0.13 | 6.6 ± 0.6 | 10.8 ± 0.4 | MDA | 0.17 ± 0.01 | 3 |
| Area-weighted cove water averages (*Alcalfar 1*) | 35.5 | 1.8 ± 0.2 | 15 ± 2 | 14 ± 3 | 6.9 ± 1.2 | | 1, 2, 3 |
| *Alcalfar 2 (February 2006)* | | | | | | | |
| Groundwater samples | | | | | | | |
| sp4 | 25.7 | 7.9 ± 1.4 | 58 ± 5 | 21.5 ± 0.9 | 18 ± 2 | 0.83 ± 0.09 | |
| Pz1-und (45 cm) | 24.2 | 18 ± 2 | 235 ± 16 | 20.2 ± 1.0 | 91 ± 4 | 4.5 ± 0.3 | |
| Pz2-beach (45 cm) | 24.2 | 33 ± 3 | 108 ± 9 | 18.2 ± 0.7 | 58 ± 2 | 3.2 ± 0.2 | |
| N well | 3.2 | 2.8 ± 0.3 | 46 ± 2 | 38.3 ± 0.9 | 53 ± 2 | 1.38 ± 0.06 | |
| Surface cove water samples | | | | | | | |
| s16 | 36.3 | 1.7 ± 0.3 | 12.3 ± 1.1 | 5.7 ± 0.3 | 8.2 ± 0.8 | 1.4 ± 0.2 | 1 |
| s17 | 36.7 | 2.5 ± 0.3 | 13.1 ± 1.4 | 9.3 ± 0.2 | 6.1 ± 0.4 | 0.66 ± 0.05 | 1 |
| s18 | 37.4 | 2.1 ± 0.2 | 11.7 ± 1.4 | 10.4 ± 0.5 | MDA | 0.18 ± 0.01 | 1 |

**Table 1** continued

| | Sal | $^{223}$Ra | $^{224}$Ra | $^{226}$Ra | $^{228}$Ra | $^{228}$Ra/$^{226}$Ra | Box |
|---|---|---|---|---|---|---|---|
| s19 | 34.7 | 2.0 ± 0.2 | 23 ± 2 | 10.1 ± 0.4 | 6.1 ± 0.6 | 0.61 ± 0.06 | 1 |
| s20 | 33.1 | 2.9 ± 0.3 | 23.3 ± 1.3 | 8.0 ± 0.3 | 9.3 ± 0.7 | 1.16 ± 0.09 | 2 |
| s21 | 30.5 | 2.1 ± 0.2 | 35 ± 2 | 8.4 ± 0.3 | 11.8 ± 0.6 | 1.41 ± 0.09 | 2 |
| s22 | 38.0 | 0.9 ± 0.3 | 10.0 ± 1.0 | 11.9 ± 0.4 | 2.5 ± 0.4 | 0.21 ± 0.03 | 2 |
| s23 | 37.6 | 1.8 ± 0.2 | 11.6 ± 0.9 | 5.2 ± 0.3 | 3.9 ± 0.4 | 0.76 ± 0.09 | 3 |
| s24 | 37.6 | 1.6 ± 0.2 | 8.5 ± 1.0 | 3.8 ± 0.3 | 4.7 ± 0.8 | 1.2 ± 0.2 | 3 |
| Area-weighted cove water averages *(Alcalfar 2)* | 36.3 | 1.8 ± 0.3 | 15 ± 4 | 6.7 ± 0.9 | 5.6 ± 1.5 | | 1, 2, 3 |
| Area-weighted total cove water averages | 36.7 | 1.2 ± 0.2 | 10.3 ± 1.2 | 10.6 ± 1.4 | 5.1 ± 1.2 | 0.47 ± 0.13 | 1, 2, 3, 4, 5, 6 |

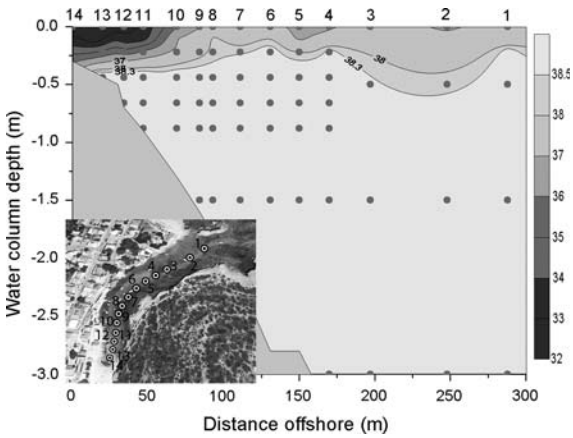


**Fig. 3** Salinity profiles offshore and at depth in 2007. A band of 50 m wide is predominantly affected by a fresher shallow (30 cm) layer of SGD flowing. Note that vertical scale is exaggerated

Considering only the area sampled during both Alc1 (May 2005) and Alc2 (February 2006), area-corrected average radium activities showed no statistical difference for $^{223}$Ra, $^{224}$Ra and $^{228}$Ra, while average activities of $^{226}$Ra were noticeably lower during Alc2 (February 2006, Table 1). Moreover, average cove water salinities for the overlapped area in May 2005 (35.4 ± 1.4) and February 2006 (35.8 ± 2.6) did not show statistical difference either. We therefore combined the data to estimate a single and consistent value of SGD. Indeed, a comparison of total rainfall in the 12 months preceding the May 2005 (Alc1; 469 mm) and February 2006 (Alc2; 493 mm) samplings shows that rainfall differences are quite small (5%).

Bottom cove water samples collected in May 2005 (*Ra1-p5*, *-p6* and *-p10*; Table 1) had salinities and $^{226}$Ra and $^{228}$Ra activities similar to seawater (37.6–37.8 compared to 38.1 and Table 1) $^{223}$Ra and $^{224}$Ra activities in near bottom waters, however, were slightly elevated above seawater (1.0 ± 0.1 against 0.6 ± 0.1 dpm 100 l$^{-1}$ for $^{223}$Ra and 5.0 ± 1.5 against 2.2 ± 0.6 dpm 100 l$^{-1}$ for $^{224}$Ra).

Groundwater samples from the fresh wells and brackish springs were enriched in radium activities (3–8 dpm 100 l$^{-1}$ for $^{223}$Ra, 36–67 dpm 100 l$^{-1}$ for $^{224}$Ra, 14–42 dpm 100 l$^{-1}$ for $^{226}$Ra and 17–52 dpm 100 L$^{-1}$ for $^{228}$Ra) relative to coastal and open seawater samples (averages of 0.6 ± 0.1, 2.2 ± 0.6, 13.3 ± 1.6 and 5.2 ± 0.8 dpm 100 l$^{-1}$, respectively) (Table 1). Wells contained especially high radium activities for the long-lived isotopes, whereas submarine springs showed a greater enrichment in the short-lived isotopes. The highest concentrations of $^{223}$Ra, $^{224}$Ra and $^{228}$Ra were obtained from the piezometer (*Pz1-und*), which had the same salinity as the springs (Table 1) and reached Ra activities as high as 235 ± 15 dpm 100 l$^{-1}$ for $^{224}$Ra, 18 ± 2 dpm 100 l$^{-1}$ for $^{223}$Ra and 91 ± 4 dpm 100 l$^{-1}$ for $^{228}$Ra. For $^{226}$Ra, the highest activities were measured in the *P1* and *P2 wells*.

## Radon concentrations

The results from water samples analyzed for $^{222}$Rn are shown in Table 2. Radon concentrations in cove waters are strongly dependent on the position and depth of the sampling station. For example, the uppermost waters (upper 25 cm) (*Rn4*) are highly enriched in radon relative to the very low radon activities measured at depth, near the sediments (*Rn1* and *Rn2*). It should also be noted here that the measured radon activities, especially the surficial

**Table 2** Radon concentrations in surface, bottom and groundwater samples

| Sample code | $^{222}$Rn (Bq m$^{-3}$) | Method | Depth (cm) |
|---|---|---|---|
| Rn4 (surficial) | 725 ± 38 | RAD AQUA | 10 cm below water's level |
| Rn1 (deep) | 28 ± 5 | RAD AQUA | 15 cm above sediment |
| Rn2 (bottom) | 9 ± 4 | RAD AQUA | 15 cm above sediment |
| sp2 (spring) | 2,450 ± 78 | RAD AQUA | Cove's water level |
| N well | 1,859 ± 734 | RAD-$H_2O$ | |
| Pz1-und | 2,696 ± 554 | RAD-$H_2O$ | 45 cm |
| Pz2-beach | 512 ± 354 | RAD-$H_2O$ | 45 cm |

sample, are likely minimum estimates, given the expected escape of the radon produced in the water column to the atmosphere. Higher to similar $^{222}$Rn activities (and salinity) were determined in groundwater obtained from the piezometer beneath the cove waters (*Pz1-und*) and from the karstic springs (*sp2*). In addition, radon levels in the fresh *N well* were also comparable to previous groundwater measurements even though salinity did differ. The piezometer on the beach (*Pz2-beach*) yielded much lower radon concentrations.

### Nutrients

Inorganic nutrient concentrations in surface stations and wells (Alc3, November 2007) are given in Table 3. Phosphate concentrations were typically low within surface waters, ranging from 0.07 to 0.41 μmol l$^{-1}$ of $PO_4^{3-}$. Concentrations of DIN (largely comprised of nitrate) and $SiO_4^{4-}$ ranged from 18 to 105 μmol l$^{-1}$ of N-DIN and from 3.5 to 16.0 μmol l$^{-1}$ of Si–$SiO_4$. N-DIN values exceeded the median concentrations measured around Minorca Island during the water quality monitoring program of 2005 and 2006 (1.78 and 1.79 μmol l$^{-1}$, respectively; $n = 49$). High nutrient concentrations, however, are not rare in the narrow inlets of Minorca, such as Cala Blanca and Cala'n Porter, which are both strongly impacted by anthropogenic activities associated with tourism. Removing one outlier station, Q, results in area-weighted averages of 0.09 ± 0.01 μM of $PO_4^{3-}$, 32.59 ± 0.03 μM for DIN and 5.59 ± 0.02 μM for $SiO_4^{4-}$. DIN and $SiO_4^{4-}$ concentrations along the central transect decrease offshore, while phosphate concentrations did not follow any clear spatial pattern. Groundwater nutrient concentrations measured from *N well* were as much as 3, 12 and 31 times greater than surface Alcalfar Cove waters for $PO_4^{3-}$, $SiO_4^{4-}$ and DIN, respectively (Table 3).

## Discussion

In order to estimate the significance of SGD into Alcalfar Cove and its potential impact on this and other similar systems, the magnitude of the SGD must first be evaluated. Here, we use a radium mass balance approach to determine the fraction of groundwater within cove waters. From this, it is then possible to determine the input of inorganic nutrients to surface waters and its possible influence on plankton growth in the nearshore.

### Radium and groundwater sources

A significant enrichment in the short-lived radium isotopes $^{223}$Ra, $^{224}$Ra and $^{228}$Ra was observed in surficial waters of the Alcalfar Cove relative to offshore. Open ocean waters typically contain ~2 dpm 100 l$^{-1}$ of $^{228}$Ra (Schmidt and Reyss 1996; Ollivier et al. 2008) and negligible activities of the shortest-lived isotopes, $^{223}$Ra and $^{224}$Ra (Moore 2000) (Fig. 4). Given that the other possible contributors of Ra to the water column (e.g. rivers and sediments) are low (see discussion below), we attribute the relatively high activities of these Ra isotopes to SGD to the cove. A plot of the radium activities as a function of salinity in surficial waters of the cove suggests that there is a binary mixing process taking place between an enriched groundwater source and the sea (Fig. 5), i.e. (1) mixing dominates decay (outputs terms) and (2) SGD through the submarine springs is the major input of radium in cove waters (input terms).

**Table 3** Nutrient concentrations (μmol $l^{-1}$) in cove water samples and wells

| Sample code | Salinity | $PO_4^{3-}$ (±0.02) | $NH_4^+$ (±0.05) | $NO_2^-$ (±0.02) | $NO_3^-$ (±0.05) | $SiO_4^{4-}$ (±0.04) | DIN (±0.07) |
|---|---|---|---|---|---|---|---|
| A | 36.9 | 0.09 | 1.64 | 0.07 | 16.65 | 3.72 | 18.36 |
| B | 36.5 | 0.08 | 1.46 | 0.08 | 24.89 | 4.58 | 26.43 |
| C | 36.9 | 0.08 | 1.12 | 0.06 | 23.26 | 3.49 | 24.44 |
| D | 36.2 | 0.07 | 0.58 | 0.06 | 23.04 | 3.88 | 23.68 |
| E | 36.1 | 0.09 | 1.26 | 0.09 | 40.94 | 8.25 | 42.29 |
| F | 36.2 | 0.10 | 1.08 | 0.08 | 49.86 | 8.70 | 51.02 |
| G | 35.9 | 0.07 | 1.55 | 0.09 | 41.16 | 5.98 | 42.80 |
| H | 35.9 | 0.08 | 1.30 | 0.07 | 41.07 | 7.31 | 42.44 |
| I | 35.1 | 0.09 | 0.73 | 0.04 | 33.95 | 4.40 | 34.72 |
| J | 35.3 | 0.09 | 0.93 | 0.08 | 43.59 | 9.10 | 44.60 |
| K | 35.3 | 0.09 | 0.85 | 0.14 | 62.01 | 10.59 | 63.00 |
| L | 34.7 | 0.12 | 1.17 | 0.15 | 55.4 | 15.29 | 56.72 |
| M | 33.1 | 0.12 | 0.92 | 0.08 | 73.73 | 11.33 | 74.73 |
| N | 36.2 | 0.09 | 1.15 | 0.10 | 55.45 | 7.13 | 56.70 |
| O | 36.0 | 0.08 | 1.26 | 0.09 | 48.09 | 8.93 | 49.44 |
| P | 36.6 | 0.08 | 1.27 | 0.11 | 33.88 | 4.29 | 35.26 |
| Q | 28.7 | 0.41 | 18.85 | 0.31 | 85.6 | 15.95 | 104.76 |
| R | 32.6 | 0.16 | 2.43 | 0.15 | 62.22 | 8.06 | 64.80 |
| S | nm | 0.24 | 2.08 | 0.10 | 28.28 | 3.45 | 30.46 |
| N well 1 | 2.9 | 0.21 | 2.49 | 0.11 | 961.13 | 86.79 | 963.73 |
| N well 2 | 2.9 | 0.28 | 1.89 | 0.11 | 1,101.11 | 44.33 | 1,103.11 |

*nm* not measured

The longest-lived isotope ($^{226}$Ra) follows a different pattern as average cove water activities are similar to the open water values reported for the western Mediterranean Sea of $\sim$10 dpm 100 $l^{-1}$ (Masqué et al. 2002). Given that Alcalfar Cove is affected by seawater intrusion, we hypothesize that most of the $^{226}$Ra within the part of the aquifer exposed to saltwater has already been leached and removed. This is supported by the observation that $^{226}$Ra activities in the brackish submarine springs are lower than in the wells located at the freshwater portion of the aquifer. Indeed, the $^{223}$Ra/$^{226}$Ra ratio at the *N well* was 0.07 ± 0.01, matching closely the parental ratio at secular equilibrium ($^{231}$Pa/$^{230}$Th = 0.05; Rama and Moore 1996). In contrast, the average $^{223}$Ra/$^{226}$Ra ratio in the brackish springs at the Alcalfar site was as high as 0.35 ± 0.09. Such low $^{226}$Ra concentrations in karstic coastal aquifers have been previously reported by others. For example, Moore (2006) concluded that depletion in $^{226}$Ra was occurring in an aquifer supplying water to a karstic area of Sicily on the basis that the $^{223}$Ra/$^{226}$Ra ratios exceeded the expected relationship of their long-lived parents. Such leaching processes would remove all radium isotopes, but the short-lived ones regenerate quickly.

Relatively high $^{228}$Ra levels in springs and the *N well* ($^{228}$Ra/$^{226}$Ra > 1) could be explained by differences in Th/U ratios in the host carbonate rocks, e.g., $^{232}$Th could be concentrated within relatively insoluble residue (silicates, phosphates and hydroxides) left behind after dissolution of carbonate aquifer rock rich in $^{228}$Ra (Sturchio et al. 2001). Another mechanism is the preferential solubility of $^{238}$U relative to $^{232}$Th, which is more closely attached to aquifer solids or sands (Von Gunten et al. 1996; Ivanovich and Harmon 1992). These $^{232}$Th enriched particles would represent a continuous source of $^{228}$Ra to ground/pore waters. In the *P1* and *P2* wells, however, there is no evidence of enriched $^{228}$Ra activity ($^{228}$Ra/$^{226}$Ra of 0.69 ± 0.03). This suggests weak dissolution of the carbonate rock, a hypothesis in accordance with the wells' location far from the coast and where karstification and fissuring processes are not so significant.

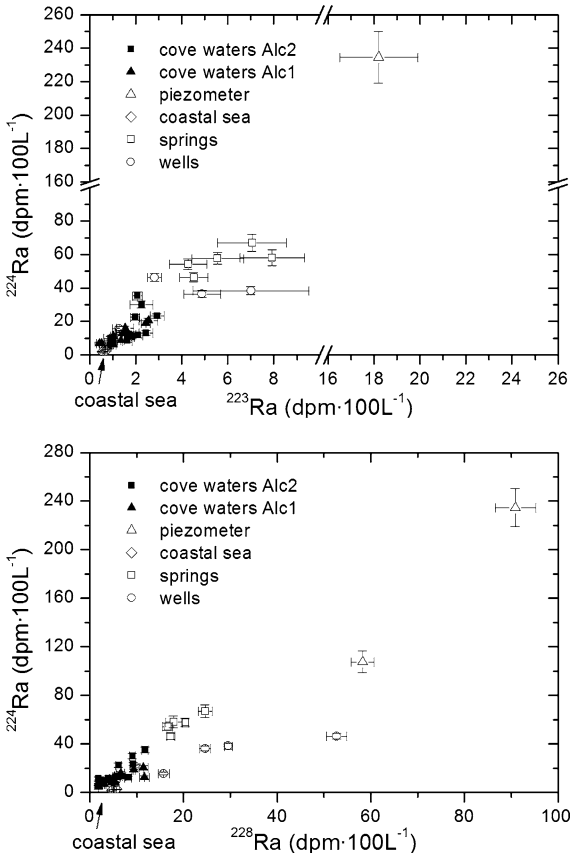


**Fig. 4** Activities of $^{224}$Ra plotted against $^{223}$Ra and $^{228}$Ra for all the water samples. A clear enrichment is detected in groundwaters respective to cove waters, which in turn are enriched compared to the immediate coastal sea

Differences in Ra enrichment between groundwaters derived from the same aquifer (greater enrichment in $^{223}$Ra and $^{224}$Ra at the springs versus higher activities of $^{226}$Ra and $^{228}$Ra in wells) may be explained by a combination of Ra desorption and dilution processes (derived from recirculation of seawater) together with the spatial distribution of the samples. For example, radium desorption is responsible for enrichment of $^{223}$Ra and $^{224}$Ra in groundwater as it moves from the fresh inner part of the aquifer to the brackish springs at the coast. In contrast, seawater intrusion dilutes the concentration of $^{226}$Ra and $^{228}$Ra. Therefore, we use the karstic springs as the brackish groundwater endmember that discharges into the cove. Given the similar $^{228}$Ra/$^{226}$Ra activity ratios ($1.2 \pm 0.4$ and $1.4 \pm 0.1$, respectively) between these brackish springs and the fresh *N well*, we hypothesize that they are derived from the same Migjorn aquifer karstified in the coastal region. These activity ratios differ from the fresh *P1* and *P2* wells because these wells are located far inland in a region dominated by carbonates.

There is a pronounced enrichment of radium activities within the porewaters of sand immersed nearshore (*Pz1-und*). The coincidence in salinity of piezometer and spring samples may indicate that in both areas, the same water seeps through the carbonate aquifer. A longer residence time (compared to the flowing karstic springs) of these porewaters could also allow for Ra enrichment. Nonetheless, there is no evidence that these enriched porewaters enter the overlying water column since radium activities within the bottom waters were much lower than in surface cove waters. $^{223}$Ra and $^{224}$Ra activities in bottom cove waters were slightly enriched relative to the surface (Table 1). We suspect that this is due to mixing of the water column nearshore followed by rapid advection.

## Ra diffusion from the sand

A sample of beach sand was analyzed by gamma spectrometry. Radium concentrations were $0.59 \pm 0.01$ dpm g$^{-1}$ for $^{226}$Ra and $0.166 \pm 0.004$ dpm g$^{-1}$ for $^{228}$Ra. These measurements suggest that radium production in situ is low as the parents (thorium) are in low concentration. However, this does not mean that Ra does not flow through the sand. Unfortunately, we do not have enough data to evaluate this mechanism directly. Rather, we can estimate Ra flow through rates by taking an upper-limit of the diffusive fluxes of $^{223}$Ra, $^{224}$Ra (0.26 and 21 dpm m$^{-2}$ day$^{-1}$, averages from control and experimental tanks containing sandy sediments, Bird et al. 1999), $^{226}$Ra and $^{228}$Ra (0.27 and 2.1 dpm m$^{-2}$ day$^{-1}$ measured in laboratory settings or reported in continental shelf sediments (Krest et al. 1999; Charette et al. 2001; Ollivier et al. 2008).

Maximum diffusive fluxes of radium (assuming the water residence time 2.4 days calculated in the following section and an average water column depth of 3 m) would explain only 1.7, 16.4, 0.2 and 3.3 of the measured $^{223}$Ra, $^{224}$Ra, $^{226}$Ra and $^{228}$Ra activities in surface cove samples. With the exception of $^{224}$Ra, the potential diffusive fluxes are thus small, and are not included in the radium mass balance delineated below. These results are similar to Burnett et al. (1990), who found uniformly low uranium-series

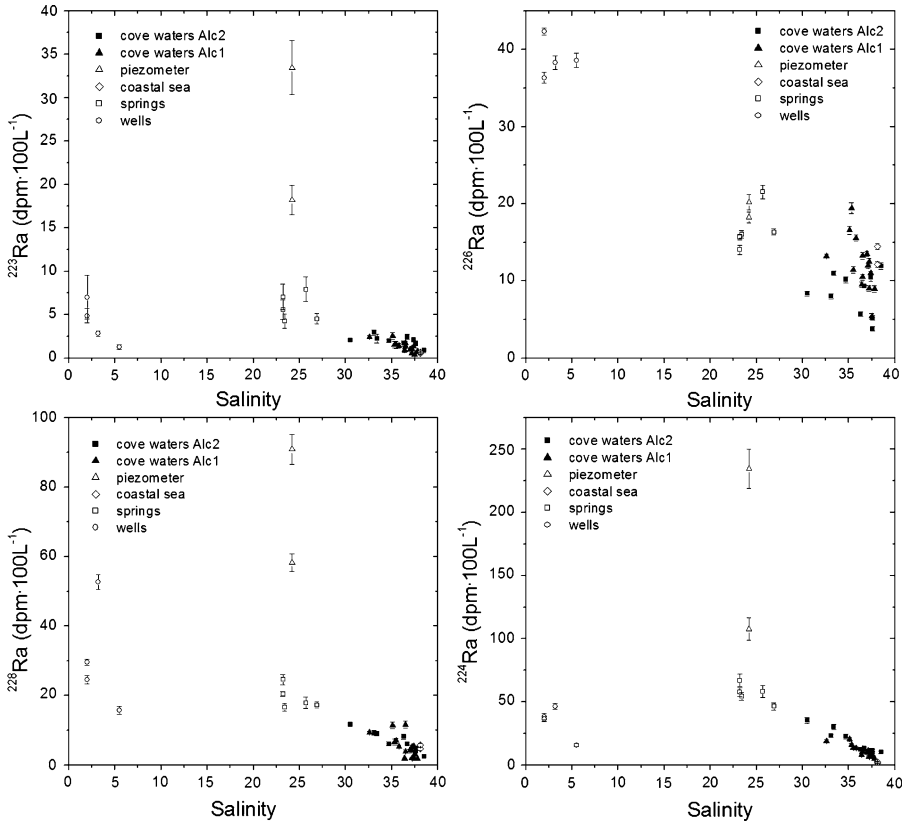


**Fig. 5** Radium activities in surficial cove waters and potential endmembers as a function of salinity

nuclide concentrations in carbonate sands and also ascribed them to negligible diffusion of radium.

## Radon as a supporting tracer

The distribution of $^{222}$Rn in bottom and surface waters confirms the layered cove water structure already observed with salinity and radium. The low radon concentration in bottom waters (*Rn1* and *Rn2*) is most likely indicative of the small amount of radium in the sediments and/or transport from other radon sources. The relatively lower radon concentrations of *Pz2-beach* suggest that brackish groundwater, which seeps from the limestone, remains stagnant beneath the beach sand and is probably not affected by active seawater recycling. This result supports the assumption of the longer residence time of sand porewater derived from high Ra activities in the *Pz2-beach* sample. The low tidal range of this area, and its protection from wave-induced mixing, would favor minimal recycling. Low radon concentrations also imply a low production of radon within the sand, which in turn suggests low adsorbed radium activities (see Ra diffusion from the sand section). The similar radon concentrations measured in the *N well*, the piezometer samples taken within the cove (*Pz1-und*) and the spring, suggest a rapid transfer of karstic groundwater to the cove. This rather high value of $\sim$2,000 Bq m$^{-3}$ is considered to be representative of the radon concentration measured in the local groundwater endmember. Therefore, the radon data obtained supports the conclusion reached above that radium diffusive fluxes are low, and that the main source of radium is groundwater flowing through the karstic limestone.

## Ra-derived cove water-mass age

The Ra released from the submarine springs can be assumed to be chemically non-reactive in cove waters and affected only by radioactive decay and mixing. The development of a Ra-derived SGD model builds

upon a mass balance of source and removal terms for radium in a coastal area, and thus relies on an estimation of the residence time of the water in the cove. The time required for a water parcel to be transported throughout a coastal region is influenced by both physical and hydrogeological factors, including tides, winds, currents and hydraulic gradients. This transit time can be calculated using physical methods, numerical models or isotopic water mass tracers (Moore 1999; Charette et al. 2001). An apparent age of water can be estimated using a Ra-based approach that compares isotopic ratios ($^{224}Ra/^{228}Ra$) in cove surface waters to measured Ra isotopic ratios in groundwater. The mathematical expression (Moore et al. 2006; Beck et al. 2007) is:

$$T = \left[F\left(^{224}Ra/^{228}Ra\right) - I\left(^{224}Ra/^{228}Ra\right)\right] / \left[I\left(^{224}Ra/^{228}Ra\right)\lambda_{224}\right] \quad (2)$$

where $F$ ($^{224}Ra/^{228}Ra$) is the $^{224}Ra/^{228}Ra$ activity ratio of the direct groundwater inputs into the system, i.e., the average activity ratio in all the sampled springs (2.9), $I$ ($^{224}Ra/^{228}Ra$) is the area-weighted average $^{224}Ra/^{228}Ra$ activity ratio in surface cove waters (2.0) and $\lambda_{224}$ is the decay constant of $^{224}Ra$ (0.1894 day$^{-1}$).

The estimated water mass age for the Alcalfar Cove waters using Eq. 2 is 2.4 days. Although water ages for the various boxes in which the cove is divided range from near 0 to 4 days, we use an average value here. We further focus on $^{224}Ra$ due to the similarity in half-life between the estimated transit time and previous hydrogeological estimates that are in the range of a few days. It is worth noticing that using Eq. 2 with $^{223}Ra/^{228}Ra$ activity ratios results in an average age of 2.5 days, in good agreement with the $^{224}Ra$ based estimate.

## Calculation of SGD using radium isotopes

Several radium-based models have been proposed to quantify SGD (Moore 2005). Here, we use a straightforward binary mixing model for the following reasons: (1) the identified coastal springs constitute the groundwater endmember from the Migjorn aquifer discharging to the cove; (2) there is a negligible tidal influence in the study site, as in most Mediterranean coastal areas; and (3) the cove waters are stratified showing clear salinity (density) gradients.

Therefore, we can define a radium mass balance where radium activities in cove waters are explained by a binary mixing of brackish groundwater and seawater endmembers. Specifically, we use the distribution of $^{223}Ra$ and $^{224}Ra$ activities combined with the $^{228}Ra/^{226}Ra$ activity ratios measured in the upper confined 30 cm ($h = 0.3$ m) of the water column. The following equations are used to establish the two end-member model at steady state:

$$f_{cs} + f_{gw} = 1 \quad (3)$$

$$^{223}Ra_{cs} \cdot f_{cs} + {}^{223}Ra_{gw} \cdot f_{gw} = {}^{223}Ra_{cove} \cdot e^{\lambda_{223} T} \quad (4)$$

$$^{224}Ra_{cs} \cdot f_{cs} + {}^{224}Ra_{gw} \cdot f_{gw} = {}^{224}Ra_{cove} \cdot e^{\lambda_{224} T} \quad (5)$$

$$\left(\frac{^{228}Ra}{^{226}Ra}\right)_{cs} \cdot f_{cs} + \left(\frac{^{228}Ra}{^{226}Ra}\right)_{gw} \cdot f_{gw} = \left(\frac{^{228}Ra}{^{226}Ra}\right)_{cove} \quad (6)$$

where $f$ is the fraction of coastal sea (cs) and groundwater (gw) endmembers in cove waters, $Ra_{cs}$ is the radium activity in the coastal seawater endmember (*sea 2* sample), $Ra_{gw}$ is the average radium activity in brackish springs and $Ra_{cove}$ is the average radium activity measured in surface cove waters. The $^{228}Ra/^{226}Ra$ terms are the activity ratios of the long-lived radium isotopes in the coastal sea, spring groundwater and cove waters. T is the apparent cove waters age (2.4 days) as estimated above.

The system of equations describing the mixing model has only two unknowns ($f_{cs}$ and $f_{gw}$) and thus three different equations for $f_{cs}$ and $f_{gw}$ can be obtained (Table 4). The average groundwater fraction in cove waters is $20 \pm 6\%$ ($f_{gw} = 0.20 \pm 0.06$). Since submarine springs are brackish, the calculated groundwater fraction will include a significant component of recirculated coastal seawater, i.e. the obtained $f_{gw}$ is a composite of $f_{gw,fresh}$ and $f_{gw,cs}$. As discussed above, the fresh groundwater (*N well*) also comes from the same Migjorn aquifer, but is salinized as it flows toward the coast where it discharges via brackish submarine springs. Although short-lived isotopes are not yet completely enriched in the fresh groundwater, we can apply the $^{228}Ra/^{226}Ra$ activity ratio of *N well* in Eq. 6. This approach yields a fresh groundwater fraction ($f_{gw,fresh}$) of 0.14. This result is probably subject to a higher uncertainty than the total groundwater fraction because several coastal wells should ideally be analyzed in order to obtain a more

**Table 4** Coastal sea and groundwater fractions derived from the use of the radium mixing model. The spring-derived groundwater fraction (0.20) includes both fresh and saline components of SGD, while the fresh well provides only with the fresh portion

| Applied equations | Isotopes | gw endmember | $f_{cs}$ | $f_{gw}$ |
|---|---|---|---|---|
| 3 and 4 | 223 | Spring | 0.84 | 0.16 |
| 3 and 5 | 224 | Spring | 0.74 | 0.26 |
| 3 and 6 | 228, 226 | Spring | 0.83 | 0.17 |
| Average | | | $0.80 \pm 0.06$ | $0.20 \pm 0.06$ |
| 3 and 6 | 228, 226 | Well | 0.86 | 0.14 |
| Total $f_{gw}$ | | | | 0.20 |
| Fresh $f_{gw,fresh}$ | | | | 0.14 |
| Recirculated $f_{gw,cs}$ | | | | 0.06 |

representative groundwater endmember. Unfortunately, there are only a limited number of wells in our coastal area. From these results, we infer that surface cove waters consist of 80% coastal seawater and 20% SGD, which further includes 14% fresh groundwater and 6% recirculated seawater.

The total submarine groundwater discharge rate (cm $day^{-1}$) within the cove is then determined by taking into account the groundwater fraction ($f_{gw} = 0.20 \pm 0.06$), the water column under study that is enriched in radium isotopes ($h$) and the calculated water apparent age ($T$) as follows:

$$\text{SGD}\left(\text{cm day}^{-1}\right) = \frac{f_{gw} \cdot h}{T} \quad (7)$$

Instead of depth ($h$), length may be used in other settings such as homogeneous coastal aquifers considered to discharge groundwater along the entire coastline and described by a well mixed water column. By solving Eq. 7, we estimate a SGD flux within the studied cove of $2.5 \pm 0.7$ cm $day^{-1}$ containing 30% recirculated seawater and 70% fresh groundwater. This linear discharge rate is multiplied by the studied Alcalfar Cove area to come up with the volumetric SGD rate of $150 \pm 43 \times 10^3$ $m^3$ $year^{-1}$, which is divided in $45 \pm 13 \times 10^3$ $m^3$ $year^{-1}$ of recirculated seawater and $105 \pm 30 \times 10^3$ $m^3$ $year^{-1}$ of fresh SGD.

The estimated SGD flux for the Alcalfar Cove (coastline of 620 m) can be extrapolated to the entire karstic shoreline of the Migjorn Aquifer (157 km), given the similarity of this cove's shape and hydrogeologic properties to other Minorca regions. Although conscious that a precise determination of the total SGD from the Migjorn aquifer would require numerous studies, we estimate that total SGD flow from the Island of Minorca is $\sim 40 \times 10^6$ $m^3$ $year^{-1}$, with 70% being fresh groundwater discharge. This latter estimate fits well within the fresh groundwater discharge calculated from a hydrological balance for the Migjorn aquifer ($17 \times 10^6$ to $37 \times 10^6$ $m^3$ $year^{-1}$; Estradé 2005). As a further test, we also used Darcy's Law to estimate the fresh SGD derive from the entire Migjorn aquifer (Freeze and Cherry 1979; Kroeger et al. 2007). The aquifer parameters involved in such a calculation are the hydraulic conductivity, the hydraulic gradient and the cross-sectional area of the plane perpendicular to flow (defined by length along shore and thickness of the aquifer). The value for the hydraulic conductivity was obtained from a detailed study by Fayas (1982), who examined more than 125 wells and concluded that hydraulic conductivities for the studied geologic formation in coastal areas were generally higher than 20 m $day^{-1}$ (K). We chose this lower-limit as a conservative, low estimate for goundwater flow. The hydraulic gradient was calculated from the latest available piezometric map (0.002 m $m^{-1}$; López-García 2004). According to Fayas (1982), the depth of the permeable aquifer formation ranges between 10 and 50 m, so that we used the average thickness of 30 m. The length of the total karstic shoreline (157 km) was calculated directly from the geologic map. Assuming these values, the calculation leads to a fresh SGD flux of $58 \times 10^6$ $m^3$ $year^{-1}$, which is higher but still comparable to the Ra-derived fresh SGD rate.

## Groundwater-derived flux of nutrients

The examination of $PO_4^{3-}$, DIN and $SiO_4^{4-}$ concentrations as a function of salinity (Table 3) suggests that that the fresh groundwater endmember is a major

source of these dissolved inorganic nutrients to the cove. In general terms, high DIN concentrations in groundwater may be associated with large pools of $NO_3^-$ and high rates of remineralization in upland soils (Street et al. 2008). However, human activities also alter N concentrations in groundwater. In this region, groundwater nitrate may also originate from fertilizers and manure, since 47% of the local land surface is devoted to agricultural and farming uses (Carreras et al. 2002).

Using the fresh SGD derived from Ra, we can estimate the groundwater associated input of new nutrients to the Alcalfar Cove by simply multiplying the fresh SGD rate by the average *N well* groundwater concentration of nutrients (Table 3), such that fresh SGD accounts for 18,000 μmol $m^{-2}$ $day^{-1}$ of $NO_3^-$, 1,140 μmol $m^{-2}$ $day^{-1}$ of $SiO_4^{4-}$ and 4 μmol $m^{-2}$ $day^{-1}$ of $PO_4^{3-}$. Using an average groundwater $NO_3$ concentration of 738 ± 190 μmol $l^{-1}$, derived from several freshwater well measurements in the region during November 2004, May–June 2006 and February 2007 ($n = 6$; Health Authorities of the Minorca Insular Government, unpublished data), the estimated $NO_3^-$ flux is 13,000 μmol $m^{-2}$ $day^{-1}$. This value, 28% lower than the above estimate, is more integrative of the seasonal and yearly variability likely to occur with $NO_3^-$ groundwater concentrations. The measured inventories of nutrients in surface Alcalfar Cove waters in November 2007 (average nutrient concentrations times the studied cove volume) are $1{,}500 \times 10^5$ μmol $NO_3^-$, $280 \times 10^5$ μmol $SiO_4^{4-}$ and $4.5 \times 10^5$ μmol $PO_4^{3-}$, which can be compared to the nutrient supply from the fresh SGD. The latter can be estimated by multiplying the SGD-associated nutrient flux (mass per time per area) by cove surface area (1.65 ha) and the cove water residence time (i.e., the time during which these waters are receiving and accumulating the input of nutrients from SGD before being exchanged by offshore seawaters). The obtained values are $7{,}100 \times 10^5$ μmol of $NO_3^-$, $450 \times 10^5$ μmol of $SiO_4^{4-}$ and $1.7 \times 10^5$ μmol of $PO_4^{3-}$. Assuming that the fresh SGD estimated from May 2005 and February 2006 is valid for November 2007, we calculate that fresh SGD supplies nearly two and five times more $SiO_4^{4-}$ and $NO_3^-$, respectively, than the inventories actually measured in cove waters. In contrast, cove $PO_4^{3-}$ inventories are almost threefold higher than the estimated fresh groundwater contribution.

While subject to significant uncertainty, the difference between groundwater supplied and observed nutrient inventories likely reflect biogeochemical transformations that occur during groundwater flow to coastal waters. These include transformation, removal or release of $NO_3^-$, $SiO_4^{4-}$ and $PO_4^{3-}$ compounds at the freshwater seawater interface (Dahm et al. 1998), as well as rapid biological utilization. For example, under oxic conditions, dissolved $PO_4^{3-}$ is generally quickly removed from groundwater through co-precipitation with dissolved Ca, Al or Fe into mineral phases such as hydroxyapatite ($Ca_5(PO_4)_3(OH)$) (Weiskei and Howes 1992; Zanini et al. 1998). This latter process could explain the lower $PO_4^{3-}$ concentrations driven by groundwater. The estimated input of $SiO_4^{4-}$ could be taken up by diatoms that require Si to build their cell walls (Rabalais et al. 2002). As for $NO_3^-$, denitrification is an important removal process for groundwater nitrogen under anoxic conditions, but this is unlikely given the rapid groundwater flow through the karstic springs (Capone and Slater 1990). Finally, these nutrients are seasonally recycled between benthos and plankton in shallow marine ecosystems (Laws 1983).

Although the rate of nutrient supply (18,000 μmol $m^{-2}$ $day^{-1}$ of $NO_3^-$, 1,140 μmol $m^{-2}$ $day^{-1}$ of $SiO_4^{4-}$ and 4 μmol $m^{-2}$ $day^{-1}$ of $PO_4^{3-}$) is remarkable, it may not necessarily correlate with the rate of nutrient assimilation by phytoplankton, which depends on a variety of factors such as light availability, plankton nutritional preferences, uptake capabilities and growth rates (Smayda 1997). Community composition may be further impacted by atomic nutrient ratios; as N:Si and P:Si ratios increase substantially in coastal areas affected by human stresses (Justic et al. 1995a, b; Slomp and Cappellen 2004 and references within). Atomic DIN:P, Si:P and Si:DIN ratios in surface waters of the Alcalfar Cove (Fig. 6) indicate probable stoichiometric P limitation in all cases (Justic et al. 1995b). Previous research has also demonstrated that phosphorus generally limits phytoplankton development in karst areas (Tapia González et al. 2008). One of the main reasons is the rapid precipitation of phosphorus in the form of apatite (calcium phosphate), which is similar to calcium carbonate (Fourqurean et al. 1993). Conversely, N and Si concentrations and ratios were high enough to allow phytoplankton growth.

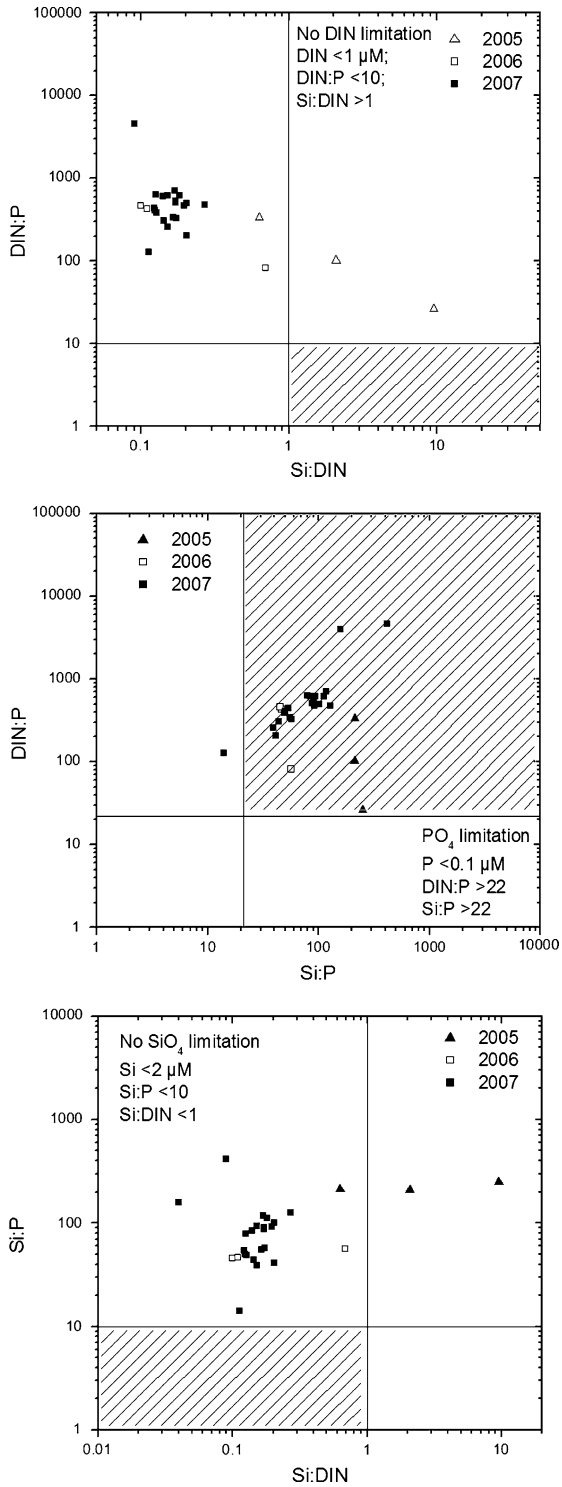


**Fig. 6** Atomic DIN:P, Si:P and Si:DIN ratios in the surface waters of the Alcalfar Cove. The areas of N, Si and P limitation are marked as well

Phytoplankton blooms, as indicated by chlorophyll a data, have been observed in Alcalfar Cove during summer, and a study of the distribution of dinoflagellates around Minorca Island from 2005 to 2006 reveals that the Alcalfar Cove had the highest cell abundance of *Gymnodinium chlorophorum* among all of the sampled coves ($n = 21$) with an abundance of $>10^6$ cell $l^{-1}$ in 2006 (Illoul et al. 2007). This phytoplankton biomass could reasonably be sustained by the consumption of nutrients derived from SGD into the system, although there are other essential factors for bloom manifestations (Basterretxea et al. 2005). Therefore, further studies need to be conducted in order to establish the exact role that SGD plays in Alcalfar Cove phytoplankton blooms.

## Conclusions

This study demonstrates the effectiveness of radium isotopes in estimating SGD rates in a karstic coastal area in the Balearic Islands (western Mediterranean). The groundwater source to this system is most likely the surficial karst aquifer, which is altered by dissolution processes that are reflected within coastal spring discharge. The $^{224}Ra/^{228}Ra$ distribution can be used to constrain a mean cove water residence time of 2.4 days. Using a radium mass balance (using $^{223}Ra$, $^{224}Ra$ and the $^{228}Ra/^{226}Ra$ ratio), SGD is calculated and separated into two components: recirculated seawater ($45 \pm 13 \times 10^3$ $m^3$ $year^{-1}$) and fresh groundwater ($105 \pm 30 \times 10^3$ $m^3$ $year^{-1}$). Radium derived fresh SGD rates yield $NO_3^-$, $SiO_4^{4-}$ and $PO_4^{3-}$ fluxes of 18,000, 1,140 and 4 µmol $m^{-2}$ $day^{-1}$, respectively, and are likely minimum estimates for total N, Si and P inputs because organic nutrients were not measured. The inorganic nitrogen and silica fluxes alone are substantial enough to promote the recurrent phytoplankton blooms observed in the area, although phosphorus limitation may occur, as in other karstic regions. Since a number of non-conservative biogeochemical processes may alter nutrient distribution in the subterranean estuary prior to SGD to the coast, concerted efforts on identifying the SGD endmember for nutrients should be undertaken, especially in areas where the proliferations of algal species may be linked to SGD.

**Acknowledgements** We gratefully acknowledge F. Garcia-Olives, C. Hanfland, C. Sintes-Gomila, P. Monjo, and D. Sintes (Aigües de Sant Lluís) for their help and assistance during field work. The authors specially thank the *Laboratori de Radioactivitat Ambiental* staff for expert and fun collaboration. We also want to acknowledge R. Ventosa for her assistance with nutrient analyses. The authors are indebted to Claudia Benitez-Nelson for her valuable suggestions and her help in improving the manuscript. This project has been partially supported by the Institut Menorquí d'Estudis (IME) and the Departament d'Universitats, Recerca i Societat de la Informació of the Generalitat de Catalunya (PICS program no. 2434). Support from the Spanish Government and the Fulbright Commission for a post-doctoral fellowship to J.G.-O. (ref 2007-0516) is gratefully acknowledged. Support for the research of PM was received through the prize "ICREA Academia", funded by the Generalitat de Catalunya.

## References

Anderson DM, Glibert PM, Burkholder JM (2002) Harmful algal blooms and eutrophication: nutrient sources, composition, and consequences. Estuaries 25(4b):704–726

Barón A, Bayó A, Fayas J (1979) Relación modelo geológico-modelo hidrogeológico. Ejemplo: el acuífero mioceno de la isla de Menorca. Act. II Simposio Nacional Hidrogeología, vol 4. Pamplona, p 19

Basterretxea G, Garcés E, Jordi A, Masó M, Tintoré J (2005) Breeze conditions as a favoring mechanism of *Alexandrium taylori* blooms at a Mediterranean beach. Estuar Coast Shelf Sci 62:1–12

Basterretxea G, Garcés E, Jordi A, Angles S, Masó M (2007) Modulation of nearshore harmful algal blooms by in situ growth rate and water renewal. Mar Ecol Prog Ser 352:53–65

Beck AJ, Rapaglia JP, Cochran JK, Bokuniewicz HJ (2007) Radium mass-balance in Jamaica Bay, NY: evidence for a substantial flux of submarine groundwater. Mar Chem 106:419–441

Bird FL, Ford PW, Hancock GJ (1999) Effect of burrowing macrobenthos on the flux of dissolved substances across the water-sediment interface. Mar Freshw Res 50: 523–532

Bourrouilh R (1983) Stratigraphie, sediméntologie et tectonique de l'île de Minorque et du Nord-Est de Majorque (Baléares). La terminaison Nord-orientale des Cordillères Bétiques en Méditerranée occidentale. Memorias del Instituto Geológico y Minero de España 99:1–672

Burnett WC, Dulaiova H (2003) Estimating the dynamics of groundwater input into the coastal zone via continuous radon-222 measurements. J Environ Radioact 69:21–35

Burnett WC, Cowart JB, Deetae S (1990) Radium in the Suwannee River and estuary. Spring and river input to the Gulf of Mexico. Biogeochemistry 10:237–255

Burnett WC, Bokuniewicz H, Huettel M, Moore WS, Taniguchi M (2003) Groundwater and pore water inputs to the coastal zone. Biogeochemistry 66:3–33

Burnett WC, Aggarwal PK, Aureli A, Bokuniewicz H, Cable JE, Charette MA, Kontar E, Krupa S, Kulkarni KM, Loveless A, Moore WS, Oberdorfer JA, Oliveira J, Ozyurt N, Povinec P, Privitera AMG, Rajar R, Ramessur RT, Scholten J, Stieglitz T, Taniguchi M, Turner JV (2006) Quantifying submarine groundwater discharge in the coastal zone via multiple methods. Sci Total Environ 367:498–543

Cable JE, Corbett DR, Walsh MM (2002) Phosphate uptake in coastal limestone aquifers: a fresh look at wastewater management. Limnol Oceanogr Bull 11(2):29–32

Capone DG, Bautista M (1985) A groundwater source of nitrate in nearshore marine sediments. Nature 313:214–216

Capone DG, Slater JM (1990) Interannual patterns of water-table height and groundwater derived nitrate in nearshore sediments. Biogeochemistry 10(3):277–288

Carreras D, Pons C, Canals A (2002) Cartografia digital de l'ocupació del territori de Menorca-2002. OBSAM-IME, Minorca. http://www.obsam.cat/documents/informes/cartografia-digital-ocupacio-territori-Menorca-2002.pdf

Charette MA, Allen MC (2006) Precision ground water sampling in coastal aquifers using a direct-push, shielded-screen well-point system. Ground Water Monit Remediat 26(2):87–93

Charette MA, Buesseler KO (2004) Submarine groundwater discharge of nutrients and copper to an urban subestuary of Chesapeake Bay (Elizabeth River). Limnol Oceanogr 49(2):376–385

Charette MA, Scholten JC (2008) Marine chemistry special issue: the renaissance of radium isotopic tracers in marine processes studies. Mar Chem 109:185–187

Charette MA, Buesseler KO, Andrews JE (2001) Utility of radium isotopes for evaluating the input and transport of groundwater-derived nitrogen to a Cape Cod estuary. Limnol Oceanogr 46:465–470

Corbett DR, Dillon K, Burnett W, Chanton J (2000) Estimating the groundwater contribution into Florida Bay via natural tracers $^{222}Rn$ and $CH_4$. Limnol Oceanogr 45: 1546–1557

Dahm CN, Grimm NB, Marmonier P, Valett HM, Vervier P (1998) Nutrient dynamics at the interface between surface waters and groundwaters. Freshw Biol 40:427–451

Estradé S (2005) Aportacions al coneixement del balanç hídric de l'aqüífer de migjorn de Menorca. OBSAM, Minorca. http://www.obsam.cat/documents/posters/Balans-hidric.pdf

Fayas JA (1972) Estudio de los recursos hidráulicos totales de la isla de Menorca. Servicio Geológico de Obras Públicas I, Madrid

Fayas JA (1982) Estudio marco para el aprovechamiento de los recursos hidráulicos de Menorca. Consell Insular de Menorca, Minorca

Fornós JJ, Obrador A, Rosselló VM (2004) Història Natural del Migjorn de Menorca, vol 11. Societat d'Història Natural de les Balears, pp 1–378

Fourqurean JW, Jones RD, Zieman JC (1993) Processes influencing water column nutrient characteristics and phosphorus limitation of phytoplankton biomass in Florida Bay, FL, USA: inferences from spatial distributions. Estuar Coast Shelf Sci 36:295–314

Freeze RA, Cherry JA (1979) Groundwater. Prentice Hall, Englewood Cliffs

Garcia-Solsona E, Garcia-Orellana J, Masqué P, Dulaiova H (2008) Uncertainties associated with $^{223}$Ra and $^{224}$Ra measurements in water via a Delayed Coincidence Counter (RaDeCC). Mar Chem 109:198–219

Garrison GH, Glenn CR, McMurtry GM (2003) Measurement of submarine groundwater discharge in Kahana Bay, O'ahu, Hawai'i. Limnol Oceanogr 48(2):920–928

Glibert PM, Burkholder JM, Graneli E, Anderson DM (2008) HABs and eutrophication. Harmful Algae 8(1):1–88

Grasshoff K, Ehrhardt M, Kremling K (1999) Methods of seawater analysis. Chapter 4: Determination of nutrients, 3rd edn. Verlag Chemie, Weinheim

Hallegraeff G (1993) A review of harmful algal blooms and their apparent global increase. Phycologia 32:79–99

Hwang DW, Kim G, Lee YW, Yang HS (2005) Estimating submarine inputs of groundwater and nutrients to a coastal bay using radium isotopes. Mar Chem 96:61–71

Illoul H, Masó M, Reñé A, Anglès S (2007) Gymnodinium chlorophorum causante de proliferaciones de altas biomasas en aguas recreativas de las islas Baleares (veranos 2004-2006). IX Reunión Ibérica sobre Fitoplancton Tóxico y Biotoxinas, Cartagena, 7–10 May 2007

Ivanovich M, Harmon RS (1992) Uranium series disequilibrium: applications to earth, marine and environmental sciences. Clarendon Press, Oxford

Justic D, Rabalais NN, Turner RE (1995a) Stoichiometric nutrient balance and origin of coastal eutrophication. Mar Pollut Bull 30:41–46

Justic D, Rabalais NN, Turner RE, Dortch Q (1995b) Changes in nutrient structure of river-dominated coastal waters: stoichiometric nutrient balance and its consequences. Estuar Coast Shelf Sci 40:339–356

Krest JM, Moore WS, Rama (1999) $^{226}$Ra and $^{228}$Ra in the mixing zones of the Mississippi and Atchafalaya Rivers: indicators of groundwater input. Mar Chem 64:129–152

Kroeger KD, Swarzenski PW, Greenwood WJ, Reich C (2007) Submarine groundwater discharge to Tampa Bay: nutrient fluxes and biogeochemistry of the coastal aquifer. Mar Chem 104:85–97

LaMoreaux PE, LaMoreaux J (2007) Karst: the foundation for concepts in hydrogeology. Environ Geol 51:685–688. doi: 10.1007/s00254-006-0378-y

Laws EA (1983) Man's impact on the marine nitrogen cycle. In: Carpenter EJ, Capone DG (eds) Nitrogen in the marine environment. Academic Press, New York, pp 459–485

López-García JM (2004) El estado de las aguas subterráneas en el archipiélago Balear. Isla de Menorca, Instituto Geológico y Minero de Esoaña. http://www.caib.es/fitxer/get?codi=185022

Maramathas A, Pergialiotis P, Gialamas I (2006) Contribution to the identification of the sea intrusion mechanism of brackish karst springs. Hydrogeol J 14:657–662

Maso M, Garcés E (2006) Harmful microalgae blooms (HAB): problematic and conditions that induce them. Mar Pollut Bull 53(10–12):620–630

Masqué P, Sanchez-Cabeza JA, Bruach JM, Palacios E, Canals M (2002) Balance and residence times of $^{210}$Pb and $^{210}$Po in surface waters of the northwestern Mediterranean Sea. Cont Shelf Res 22:2127–2146

Moore WS (1976) Sampling $^{226}$Ra in the deep ocean. Deep Sea Res 23:647–651

Moore WS (1996) Large groundwater inputs to coastal waters revealed by $^{226}$Ra enrichments. Nature 380:612–614

Moore WS (1999) The subterranean estuary: a reaction zone of ground water and sea water. Mar Chem 65:111–126

Moore WS (2000) Ages of continental shelf waters determined from $^{223}$Ra and $^{224}$Ra. J Geophys Res 105:22117–22122

Moore WS (2005) The role of submarine groundwater discharge in coastal biogeochemistry. J Geochem Explor 88:389–393

Moore WS, Arnold R (1996) Measurement of $^{223}$Ra and $^{224}$Ra in coastal waters using a delayed coincidence counter. J Geophys Res 101:1321–1329

Moore WS, Astwood H, Lindstrom C (1995) Radium isotopes in coastal waters on the Amazon shelf. Geochim Cosmochim Acta 59(20):4285–4298

Moore WS, Blanton JO, Joye SB (2006) Estimates of flushing times, submarine groundwater discharge, and nutrient fluxes to Okatee Estuary, South Carolina. J Geophys Res 111:C09006. doi:10.1029/2005JC003041

Nixon SW (1995) Coastal eutrophication: a definition, social causes, and future concerns. Ophelia 41:199–220

Ollivier P, Claude C, Radakovitch O, Hamelin B (2008) TIMS measurements of $^{226}$Ra and $^{228}$Ra in the Gulf of Lion, an attempt to quantify submarine groundwater discharge. Mar Chem 109:337–354

Paytan A, Shellenbarger GG, Street JH, Gonneea ME, Davis K, Young MB, Moore WS (2006) Submarine groundwater discharge: an important source of new inorganic nitrogen to coral reef ecosystems. Limnol Oceanogr 51:343–348

Rabalais NN, Turner RE, Dortch Q, Justic D, Bierman VJ, Wiseman WJ (2002) Nutrient-enhanced productivity in the northern Gulf of Mexico: past, present and future. Hydrobiologia 475(476):39–63

Rama M, Moore WS (1996) Using the radium quartet for evaluating ground water input and water exchange in salt marshes. Geochim Cosmochim Acta 60(23):4645–4652

Schmidt S, Reyss JL (1996) Radium as internal tracer of Mediterranean Outflow Water. J Geophys Res 101:3589–3596

Slomp CP, Cappellen PV (2004) Nutrient inputs to the coastal ocean through submarine groundwater discharge: controls and potential impact. J Hydrol 295:64–86

Smayda TJ (1997) Harmful algal blooms: their ecophysiology and general relevance to phytoplankton blooms in the sea. Limnol Oceanogr 42(5, part 2):1137–1153

Street JH, Knee KL, Grossman EE, Paytan A (2008) Submarine groundwater discharge and nutrient addition to the coastal zone and coral reefs of leeward Hawai'i. Mar Chem 109:355–376

Sturchio NC, Banner JL, Binz CM, Heraty LB, Musgrove M (2001) Radium geochemistry of ground waters in Paleozoic carbonate aquifers, midcontinent, USA. Appl Geochem 16:109–122

Sun Y, Torgersen T (1998) The effects of water content and Mn-fiber surface conditions on 224Ra measurement by 220Rn emanation. Mar Chem 62:299–306

Tapia González FU, Herrera-Silveira JA, Aguirre-Macedo ML (2008) Water quality variability and eutrophic trends in karstic tropical coastal lagoons of the Yucatán Peninsula. Estuar Coast Shelf Sci 76:418–430

Trilla J (1979) Hidrogeologia. Enciclopedia de Menorca, vol I, Ed Obra cultural Menorca, Maó, pp 239–264

UNESCO (2004) Submarine groundwater discharge. Management implications, measurements and effects. IHP-VI, Series on groundwater 5. IOC manuals and guides 44. ISBN 92-9220-006-2

Von Gunten HR, Surbeck H, Rossler E (1996) Uranium series disequilibrium and high thorium and radium enrichments in karst formations. Environ Sci Technol 30:1268–1274

Weiskei PK, Howes BL (1992) Differential transport of sewage-derived nitrogen and phosphorus through a coastal watershed. Environ Sci Technol 26:352–360

Zanini L, Robertson WD, Ptacek CJ, Schiff SL, Mayer T (1998) Phosphorus characterization in sediments impacted by septic effluent at four sites in central Canada. J Contam Hydrol 33(3–4):405–429